Die design parameters effect on dimensional conformity of PEM fuel cell bipolar plates in rotary forming of SS316L thin sheets

Asgari, A.; Zeestraten, M.; Walters, C. L.

DOI
10.1016/j.jmapro.2024.11.035

Publication date
2024

Document Version
Final published version

Published in
Journal of Manufacturing Processes

Journal of Manufacturing Processes 132 (2024) 744–758

Contents lists available at ScienceDirect

Journal of Manufacturing Processes

journal homepage: www.elsevier.com/locate/manpro

Die design parameters effect on dimensional conformity of PEM fuel cell bipolar plates in rotary forming of SS316L thin sheets

A. Asgari [a,*], M. Zeestraten [b], C.L. Walters [a]

[a] Department of Maritime and Transport Technology, Delft University of Technology, Mekelweg 2, 2628 CD Delft, the Netherlands
[b] Madern Group, Vikingbank 1, 3133 KX Vlaardingen, the Netherlands

ARTICLE INFO

Keywords:
Rotary forming
PEM fuel cell
Bipolar plates
Die design
SS316L
Sheet

ABSTRACT

Rotary forming is a promising technique for high-volume, low-cost production of fuel cell components such as bipolar plates, but it needs to be better characterized for this application. In this paper, die design parameters in rotary forming of ultra-thin stainless steel 316 L sheets 100 μm thick are evaluated to explore how channels perpendicular and parallel to the rolling direction are affected by critical forming process parameters, namely depth of deformation, die corner radius, and friction coefficient. Channels are formed experimentally, and the results are used to verify the 2D and 3D simulations. The process is analysed in terms of die movement path and forming. Stress, strain, formed shape, and thickness are compared for the two main forming directions. Results showed that channels formed parallel to the rolling direction experience more plastic deformation and conform better to the prescribed geometry in terms of channel and flatness angles.

1. Introduction

Fuel cells have become a promising clean energy conversion technique owing to lighter weight, smaller size, and easier execution compared to conventional combustion engines [1]. The fuel cell efficiency greatly depends on its bi-polar plate (BPP) design and manufacturing accuracy; BPP geometry influences structural integrity, gas distribution and electrical and thermal conductivity within the fuel cell [1]. For example, Wang et al. [2] pointed out that improved channel geometry can increase flow velocity, thus promoting waste water removal, thereby improving the cell performance. Kerkoub et al. [3] showed a trade-off involved in channel width and rib-width on the performance of fuel cells. Manso et al. [4] presented a study confirming that the channel height to width ratio affect the fuel cell performance. They indicated that higher channel height to width ratio causes more uniform current densities, heat distribution and higher water content, thus improving the performance.

To cost-effectively manufacture polar plates, a trade-off is required between achieving favourable geometry and rigorous tolerances. Leng et al. [5] studied materials and flow channel designs used in bipolar plates for fuel cells. They found that conventional forming methods are difficult for fine channels. For this reason, many researchers have been investigating other manufacturing methods for fabricating metallic fuel cell bipolar plates, such as stamping process [6], rubber pad forming [7], hydroforming [8], hot metal gas forming [9], and rotary forming [10]. Among all the methods for manufacturing bipolar plates, stamping has been most utilized because of simplicity and reliability. Tran et al. [11] studied the effect of multi-stage stamping of 80 μm thick ferritic stainless steel on the formability, springback and thickness distribution of sheets. They reported noticeable decrease in the springback and decrease in thickness reduction using a 2-stage forming owing to the attenuation of residual stresses. Modanlo et al. [12] investigated the filling depth, thinning ratio, and stress during the rubber pad forming of SS316L with a thickness of 100 μm, intended for use in fuel cell bipolar plates. Xu et al. [13] evaluated residual stress as well as thickness variation of stamped thin stainless steel. They found that with the increase of radius or curvature, more uniformity in sheet thickness was observed. Hu et al. [14] studied effects of stamping parameters such as punch speed, die radius, draft angle, and channel dimensions on the peak thinning of SS304 thin sheets. Karacan et al. [15] assessed formability of thin sheet SS304. They considered two channel widths and depths to explore their effects on the formability and critical strains. Teng et al. [16] used a two-step rubber pad forming process to fabricate the channels of fuel cell bipolar plates made of SS304. They evaluated the die geometrical parameters for structures like length, width, edge chamfer, and the height ratio in the first step of forming. Qiu et al. [17] reached correlation of

* Corresponding author.
E-mail address: a.asgari@tudelft.nl (A. Asgari).

https://doi.org/10.1016/j.jmapro.2024.11.035
Received 25 July 2024; Received in revised form 8 November 2024; Accepted 12 November 2024
Available online 16 November 2024

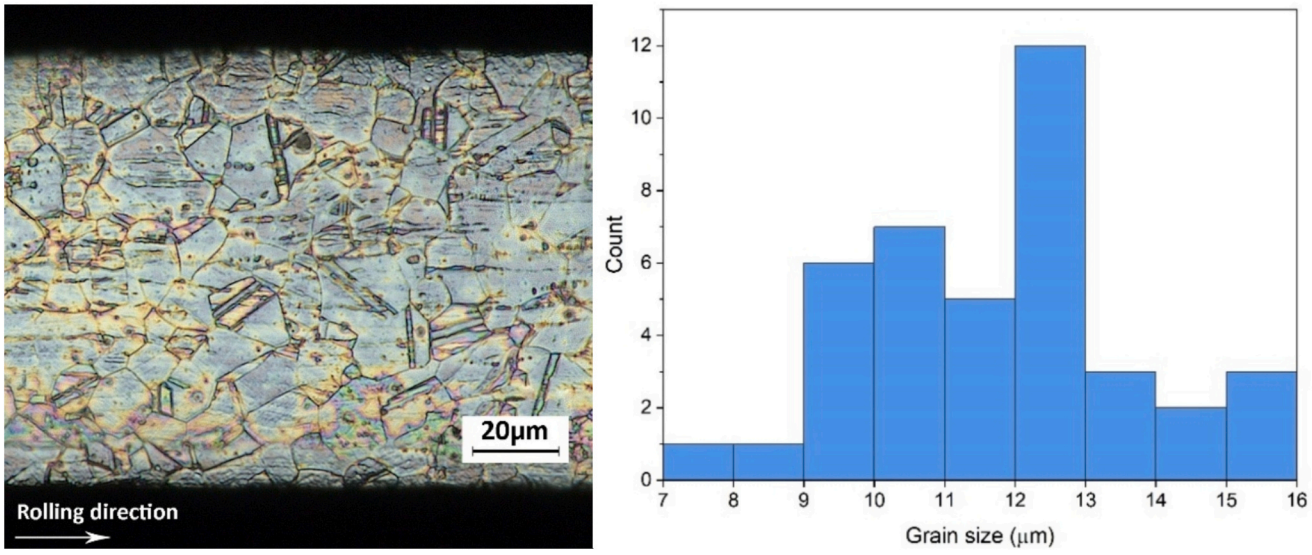

Fig. 1. Microstructure of stainless steel 316L and its grain size distribution.

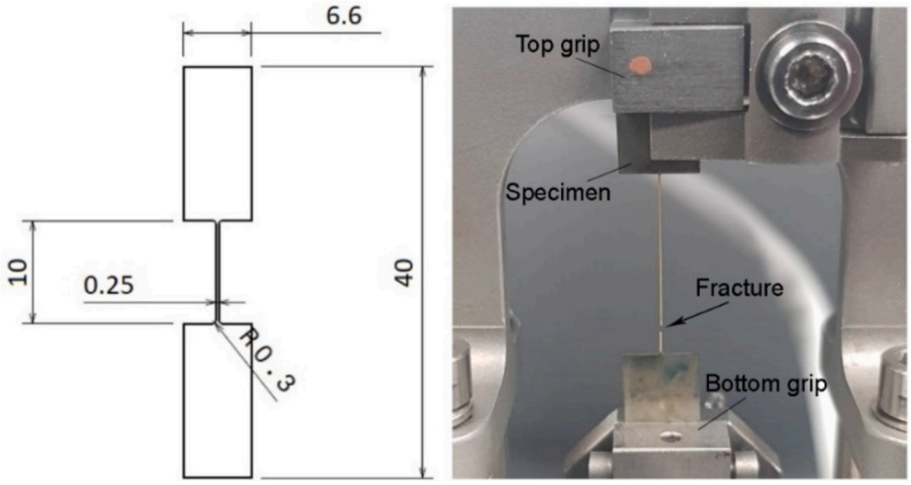

Fig. 2. Geometry of the tensile test specimen geometry (left) and configuration in the testing machine (right), dimensions are in mm.

Table 1
Cowper-Symonds parameters for stainless steel [35].

Material	C_{cs} (s^{-1})	P (–)
SS316L	240	4.74

channel forming height and process parameters such groove width, rib width, radius of die, radius of punch and clearance in stamping to obtain maximum forming height experimentally. Mahabunephachai et al. [18] investigated the effect of stamping force and hydroforming pressure on channel height and surface roughness of stainless steels SS304, SS316L, and SS430 fuel cell bipolar plates. Chen and Ye [19] analysed thickness distribution and channels height of thin SS304 steel sheets formed through micro-stamping technology with different materials model. Chen and Ye [20] investigated thickness distribution and channel height of formed stainless steel 304 in micro stamping experimentally and numerically. They analysed effects of two material models on the thickness and channel depth. Gao et al. [21] predicted deformation including equivalent von Mises stress and strains for single and triple channels of formed SS404. They pointed out that increase in the number of channels would enhance the risk of cracks in the sheet. Jin et al. [22]

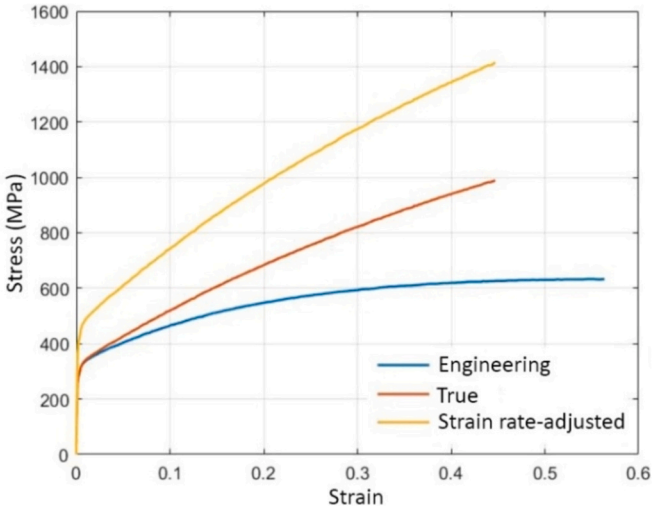

Fig. 3. Tensile test results of SS316L.

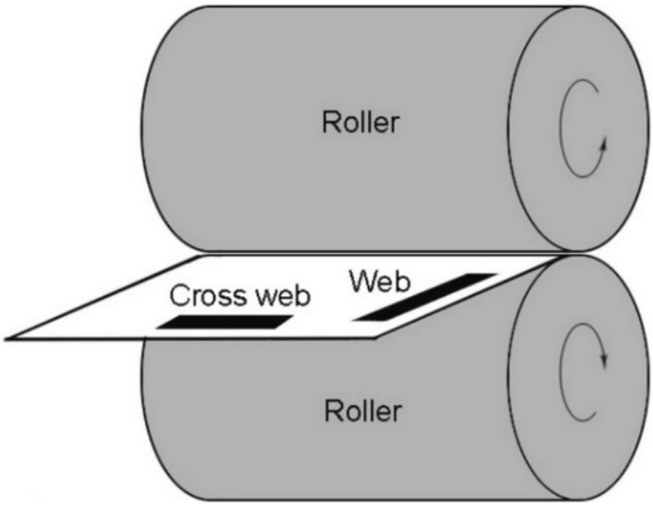

Fig. 4. Orientation of the troughs relative to the rollers.

studied effects of forming parameters on the depth of channels in fuel cell bipolar plates. Punch speed, compression pressure, rubber thickness and rubber hardness were considered in their research as forming parameters. However, the micro-stamping process has limitations in terms of production speed, energy, and cost, which drives a continued search for lower-cost, faster production methods.

Demand for mass production of fuel cells drives a transition from conventional methods to lower cost, higher rate methods. Among the most common methods used in manufacturing bipolar plates, rotary forming requires a very low fabrication time [23]. In rotary forming, two rollers containing die segments are rotated while the sheet passes between the dies. There are only a few papers published on using this process for producing bipolar plates. Nikam and Reddy [24] used two corrugators to form 250 μm thick copper sheets in web directions. They indicated that corrugated sheet bipolar plates showed excellent performance in long-term stability. Xu et al. [25] studied cold forming of AA6061-T6 with a thickness of 250 μm. They analysed the effects of forming speed, bending angle and friction coefficient on the peak plastic strain. They pointed out that the bending angle and friction coefficient are main factors affecting plastic strain. Abeyrathna et al. [26] used micro-rolling to corrugate 100 μm thick SS304L foil with four stations in the web direction. Thinning observed in the corrugating was sensitive to incorrect roll gap, tool misalignment, tool inaccuracy and surface finish of the tooling. Bauer et al. [27] studied rolling of 316 L sheet with 100 μm thickness to form channels. They found that applying strip tension reduces wrinkling and springback. Zhang et al. [28] pointed out that in micro roll forming of SS304L with 100 μm, the most thickness reduction

Fig. 5. Rotary forming setup including rollers (left) and dies (right).

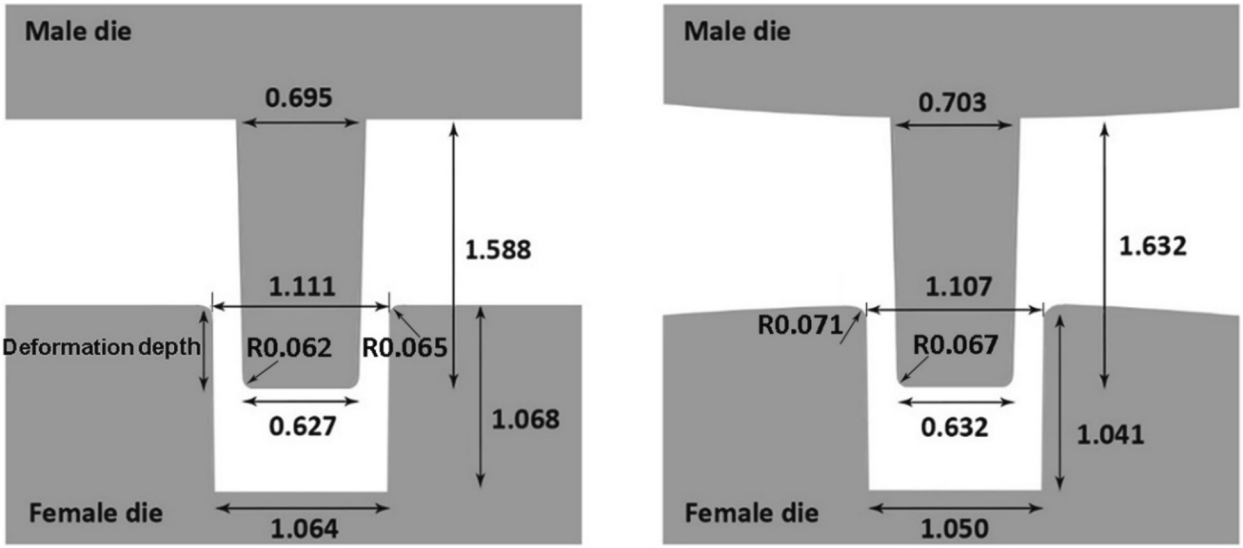

Fig. 6. Die geometries for both web and cross-web forming, dimensions in mm.

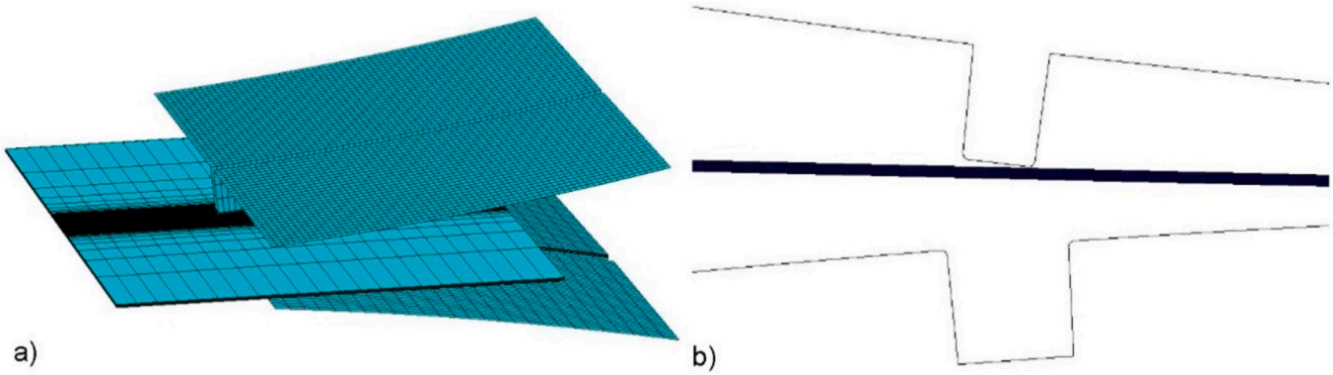

Fig. 7. Assembled meshed dies and sheet in simulation of rotary forming for two different directions, a) web direction (3D), and b) cross-web direction (2D).

Table 2
Rotary forming process parameters.

Process parameters	Unit	Value
Depth of deformation (DD)	mm	0.2, 0.33, 0.5
Corner radius (CR)	mm	0.05, 0.1, 0.15
Friction coefficient (FC)	–	0.1, 0.2, 0.3

Table 3
Design of simulations for parametric study in two cases of web and cross-web directions.

Run	Direction	DD (mm)	CR (mm)	FC (−)
1	Cross-web	0.2	0.1	0.1
2	Cross-web	0.33	0.1	0.1
3	Cross-web	0.5	0.1	0.1
4	Cross-web	0.33	0.05	0.1
5	Cross-web	0.33	0.15	0.1
6	Cross-web	0.33	0.1	0.2
7	Cross-web	0.33	0.1	0.3
8	Web	0.2	0.1	0.1
9	Web	0.33	0.1	0.1
10	Web	0.5	0.1	0.1
11	Web	0.33	0.05	0.1
12	Web	0.33	0.15	0.1
13	Web	0.33	0.1	0.2
14	Web	0.33	0.1	0.3

was observed at the areas close to the end of channel's height. Huang et al. [29] designed a pair of dies based on gear parameters to accomplish roll forming of thin SS316L. They assessed effects of fillet radius, gear tooth number and assembly errors on thickness reduction and formed channels. Xu et al. [30] studied adhesion and ploughing by modelling the friction behaviour during micro roll forming of copper (Cu-FRHC) sheet metal with the thickness of 100 μm. Ren et al. [31] used micro rolling for manufacturing of copper/SS304L micro composite channels. They analysed interfaces of composites, surface topography and roughness caused by rolling. The aforementioned research on the rotary forming of thin sheets for bipolar plates shows that there is a big gap as they only focused on a single channel direction and the process is not fully analysed in terms of die design parameters and corresponding forming mechanism. In a real bipolar plate, channels are oriented in a combination of different angles. Hence, for different channel orientations, a parametric study on the effects of key process parameters and dimensional conformity should be performed which are not studied in other studies.

In this research, the rotary forming process of SS316L sheet is assessed with a focus on analysing the die design parameters, namely: deformation depth, corner radius, and friction coefficient. Their effects on von Mises stresses and equivalent plastic strains, flatness and channel angles in loaded and unloaded conditions, and thickness distribution are systematically evaluated. All assessments are performed for different channel forming directions: formed in different directions parallel to the axis of die rotation (cross-web direction) and perpendicular to the axis of die rotation, i.e. in the direction of part travel (web direction). To this end, the forming process is modelled in 2D and 3D with an explicit nonlinear solver for cross-web and web directions, respectively. The simulations are verified by experiments by comparing thinning, channel height, channel angle, and overall shape. Then, the process parameters are varied to evaluate their influence. Finally, the importance of channel orientation along with the parameters' effects in the rotary forming of fuel cell bipolar plates are presented.

2. Materials and methods

The structure of this section approximately follows the information flow within the development. The material is first characterized, including information on both the microstructure and mechanical behaviour. After that, the forming experiments are described. Finally, the simulation methods are described.

2.1. Material characterizations

Bipolar plates are commonly manufactured from stainless steels because of the material features, such as formability, resistance to corrosion, and lack of permeability [32,33]. In the current research, stainless steel 316L with the initial thickness of 100 μm is used. To characterize the microstructure of the sheet materials, the stainless steel was mounted, polished, etched, and investigated with an optical microscope. To expose the grains, an etchant consisting of 10 mL water, 10 mL HCl, and 1 mL HNO_3 is utilized. Then, software ImageJ-1.47 was used to extract the grain size. Fig. 1 illustrates the microstructure of the material and the grain size distribution on the cross-section of sample. As can be seen, grain sizes vary from 7 to 16 μm. The average grain size is 11.74 μm, which agrees with the value reported by Guo et al. [34]. This shows that the grain size was only 11.74 % of the thickness, which supports the modelling of this material as a continuous solid in the

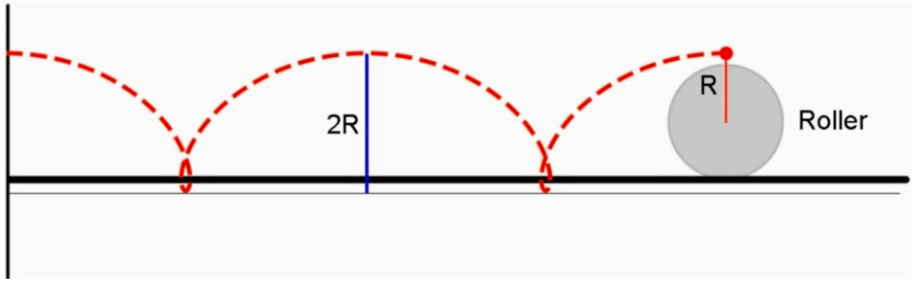

Fig. 8. Cycloid path of rollers during forming in cross-web direction.

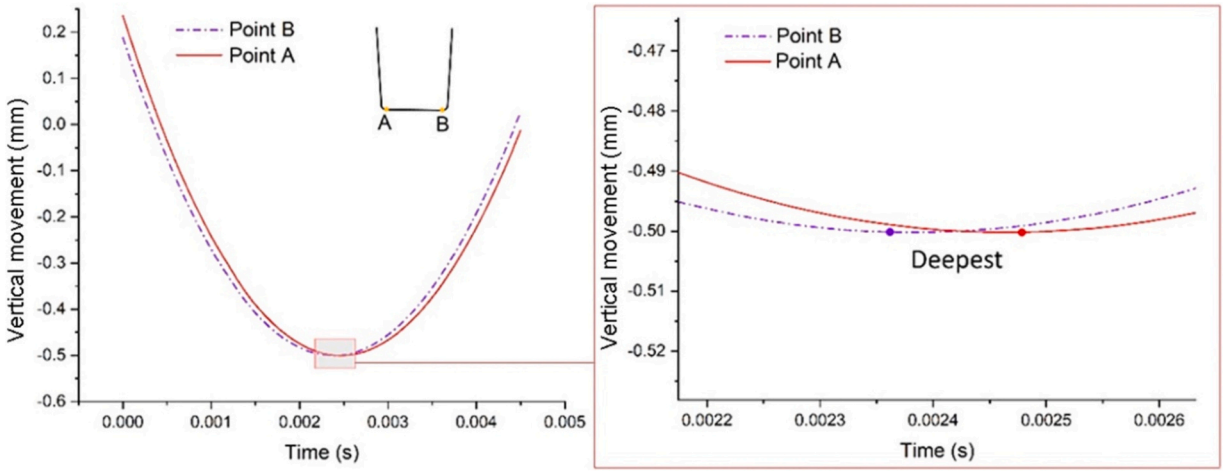

Fig. 9. Vertical movement trace of two points on the male die for forming oriented in cross web direction.

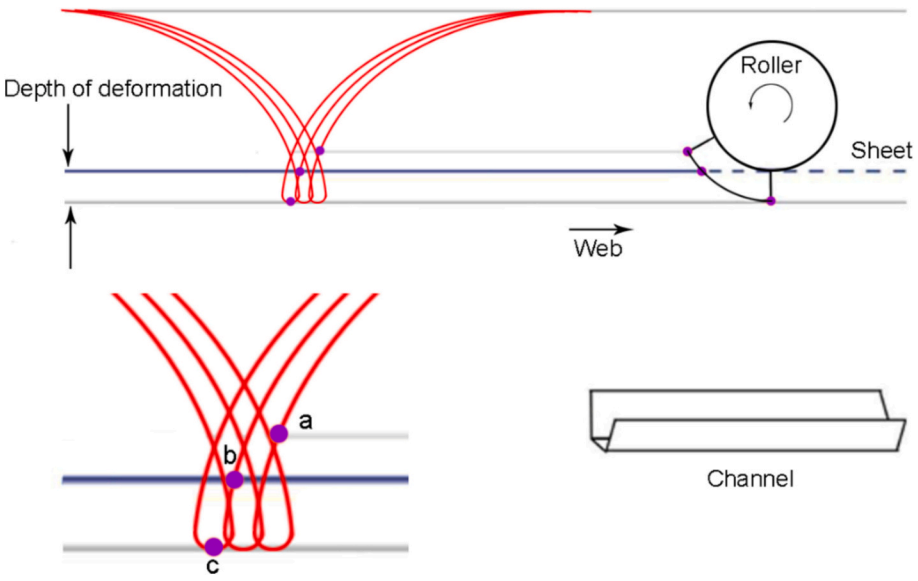

Fig. 10. Movement of points with different positions based on the extended cycloid paths.

modelling section.

Uniaxial tensile tests were performed to measure the mechanical properties of SS316 alloy sheet. The tensile tests were performed on a TA Instruments Q800 DMA machine with a capacity of 18 N. A grip speed of 200 μm/min was used, which corresponds to a strain rate of 0.0003 s^{-1} obtained by deviding the total strain by the duration. The geometry of the specimen and configuration within the testing machine are shown in Fig. 2. The rotary forming process is estimated to impose strain rate of 4.4 s^{-1} in the sheet. However, strain rate obtained by the uniaxial tensile was significantly much less than the rotary forming strain rate. Hence, the Cowper-Symonds model used to adjust the stress-strain curve for higher strain rates is presented as following equation:

$$\frac{\sigma_d}{\sigma_s} = 1 + \left(\frac{\dot{\varepsilon}}{C_{cs}}\right)^{\frac{1}{P}} \quad (1)$$

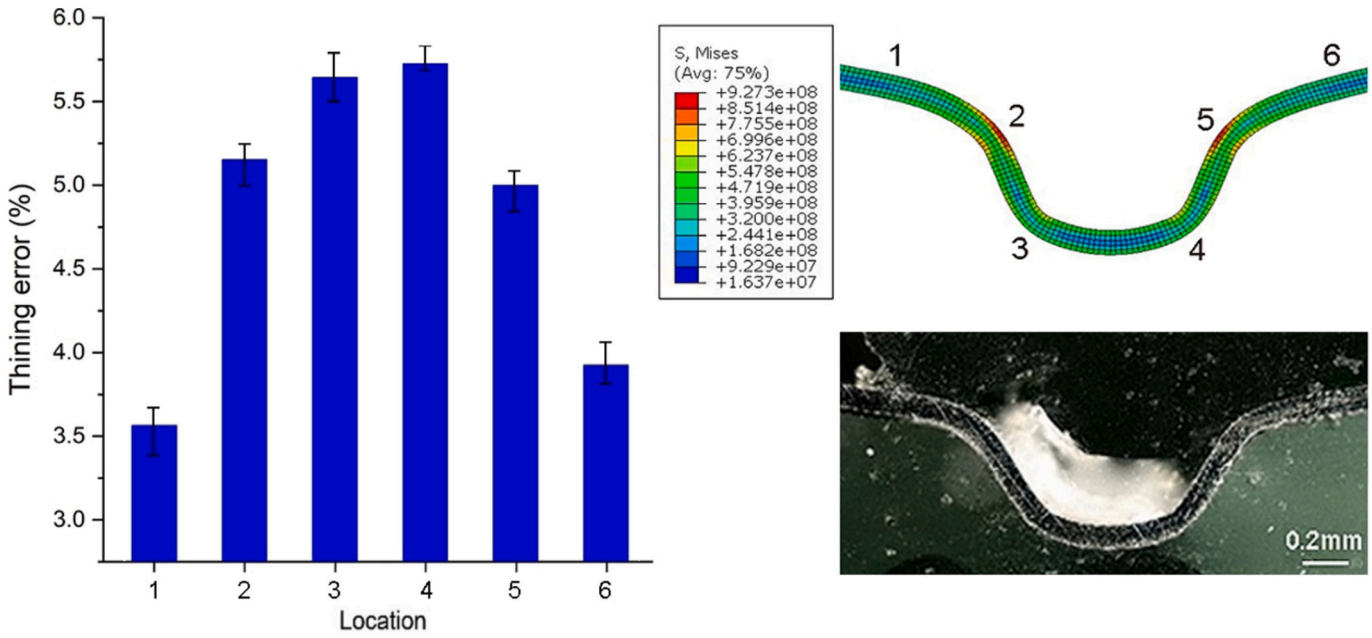

Fig. 11. Verification of modelling of rotary forming for web-direction by thinning.

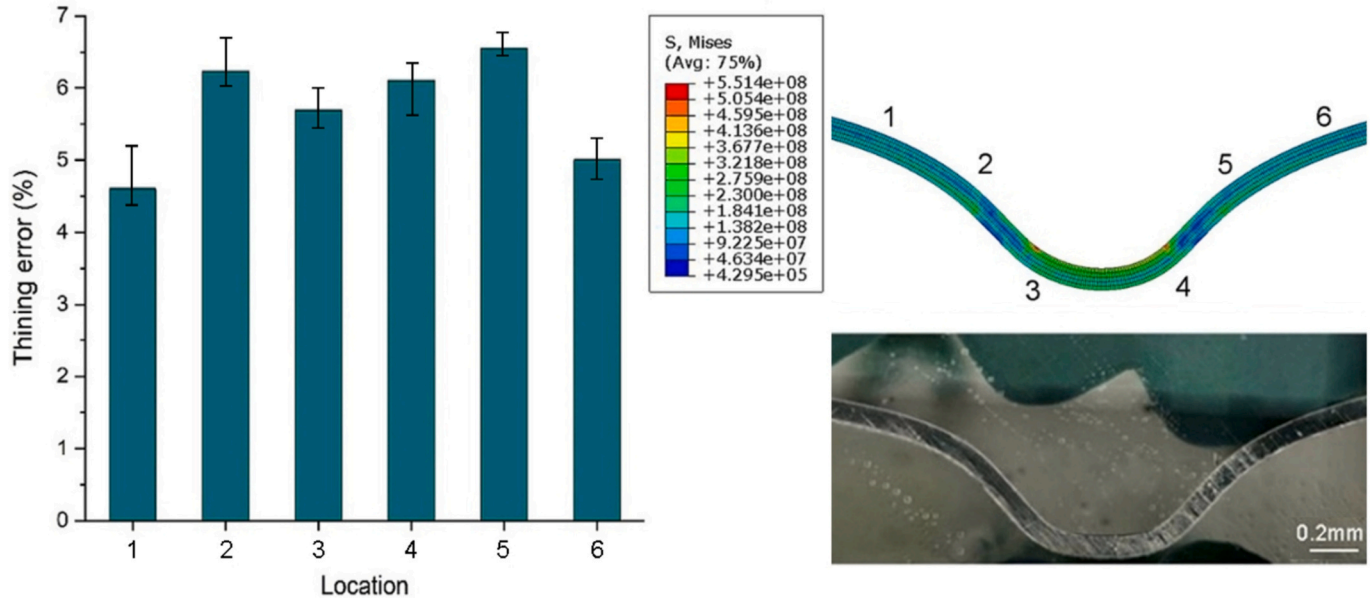

Fig. 12. Verification of modelling of rotary forming for cross-web by thinning.

where $\dot{\varepsilon}$, σ_d and σ_s are the strain rate, dynamic and static yield stresses respectively. Also, C_{cs} and P are the material constants. The constants, based on the literature [35], are presented in Table 1. To simplify the modelling, the stress-strain curve is adjusted based on the rotary forming strain rate. It should be noted that the strains in the formed sheet have roughly the same order of magnitude. The engineering and true stress-strain curves are shown in Fig. 3, along with the stress-strain curve adjusted for strain rate based on the Cowper-Symonds model. The adjusted stress-strain values are used in Abaqus to simulate the process. The stress-strain curve extracted from tensile tests indicated an appropriate agreement with the literature [36].

2.2. Forming experiments

Bipolar plates have a pattern of formed channels. These channels serve to distribute gas, dispose resulting water, and provide cooling channels. The efficiency of the cell is closely linked to the channel geometry. In most designs, there are channels perpendicular to each other. Therefore, in the current research, two dies including single channels are considered to analyze forming parameters. One of those dies is oriented in web direction, while the other one is oriented in cross-web direction, parallel to the roller axis. These two orientations are shown in Fig. 4. Besides being representative of tightly packed flow fields, the web and cross-web directions represent the extreme conditions of rotary forming.

The experiments were performed by inserting dies into a rotary

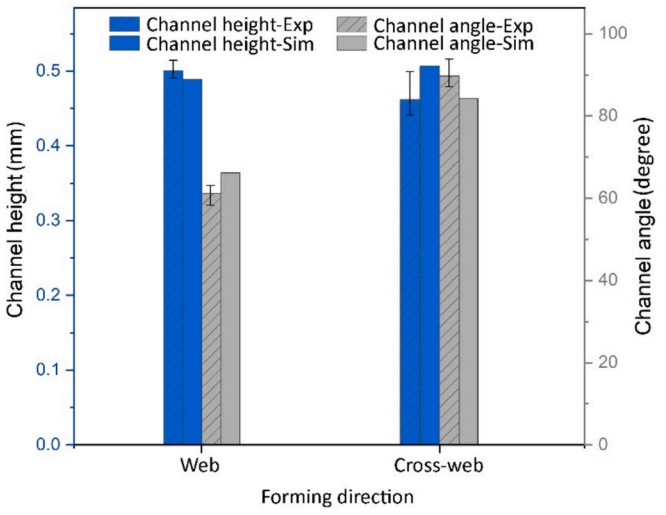

Fig. 13. Verification of modelling through channel height and angle.

forming setup. The setup and dies are shown in Fig. 5. The drums, with radius 129.28 mm, were rotated by hand at a speed of approximately one rotation per second. The sheet was inserted once they were already rotating at speed. The geometry of the male and female dies for both cases of web direction and cross-web direction are illustrated in Fig. 6. Depth of deformation was set to 0.33 mm during the experiments. Following the forming process, the specimens were cut with wire electro-discharge machining, embedded and polished for later analysis.

2.3. Finite element simulations

Finite Element Analysis (FEA) simulations were performed in Abaqus-V21 with an explicit dynamic solver. In the simulation, the sheet is modelled as a deformable solid while both male and female dies are defined as analytical rigid bodies. The dies rotate around a reference point which is coincident with the axis of rotation. The sheet is partitioned to use finer meshes in the forming zone. Fig. 7 shows the assembled dies and sheet. The simulation of the channel in the web direction used 24,200 8-node linear brick C3D8R elements with reduced integration and hourglass control. In the area of highest deformation, the minimum element edge length was 0.02 by 0.02 by 0.02 mm, such that there were 5 elements through the thickness. In the cross-web direction, 4220 4-node plane strain elements CPE4R were utilized for 2D simulation of cross-web direction. The elements were 0.01 by 0.02 mm such that there were 5 elements through the thickness.

A parametric study was performed, in which several important process parameters, namely depth of deformation, corner radius, and friction coefficient, are changed. The friction coefficient range corresponded to metallic surfaces is chosen based on the values reported in the literature [30,37]. To assess their effects, three levels of these parameters are chosen, presented in Table 2.

To reduce the number of simulations, a design for simulations is done and presented in Table 3. Seven simulations for each forming direction, thus 14 simulations in total, were carried out. It should be noted that as interaction of the die parameters was not concerned in the design, the statistical approaches like ANOVA was not used.

3. Results and discussion

The results are presented and discussed in this section. First, a critical analysis of the rotary forming process, focusing on the development of channels in both the web and cross-web direction is presented. Following that, the finite element modelling is verified against experimental results. The stress and strain fields are developed. As a measure of the conformity of final shape to die shape (i.e. indirectly measuring spring back), the angles of the channel walls and flat areas outside of the channels is presented. Finally, the thickness of the formed material is presented.

3.1. Rotary forming process analysis

In rotary forming, the orientation of channels formed by dies relative to the direction of travel is important. As a matter of fact, these relative directions define how plastic deformation is applied into the sheet. In the current study, two main directions of cross-web and web are considered for analysis of the rotary forming process. Other channel paths in a flow field of a fuel cell could somehow be a combination of the main directions. Fig. 8 shows the movement of a sample point as the rollers move; this is an extended cycloid path.

In the cross-web direction, in contrast to the conventional stamping process, two corners of a die, namely points A and B in Fig. 9, do not reach their final position at the same time. This means that when point B initially contacts the sheet, point A is yet involved in the forming process. Also, when point B approaches the final position, point A would not apply forming load to the sheet. Fig. 9 illustrates the difference between movement of point A and B according to the die geometry presented in Fig. 6.

In the web direction, the forming process is done continuously. Some of the sheet material around the material that is being formed plays the role of boundary condition. It clamps the sheet, though not completely and strictly since the sheet is deformable and there is little clamping force outside of the area being actively deformed. Fig. 10 illustrates how

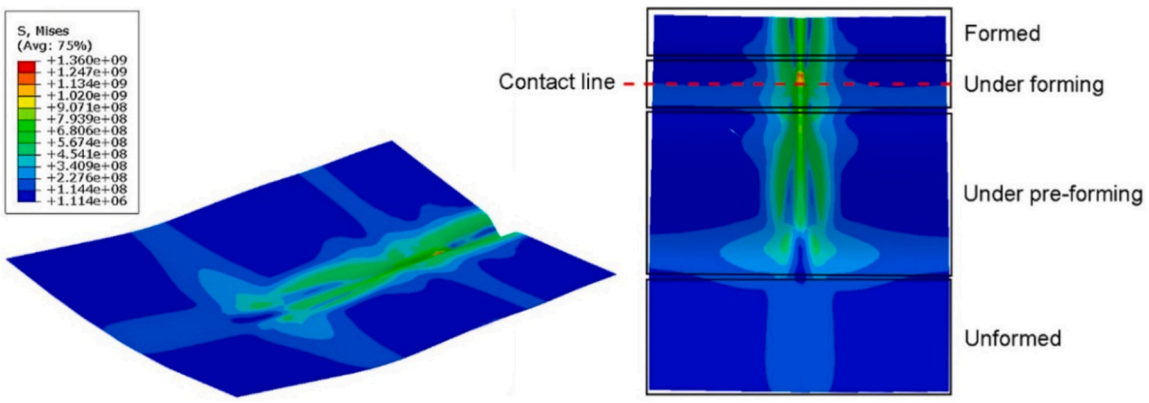

Fig. 14. Continuity in the forming of a single channel for the case oriented in web-direction.

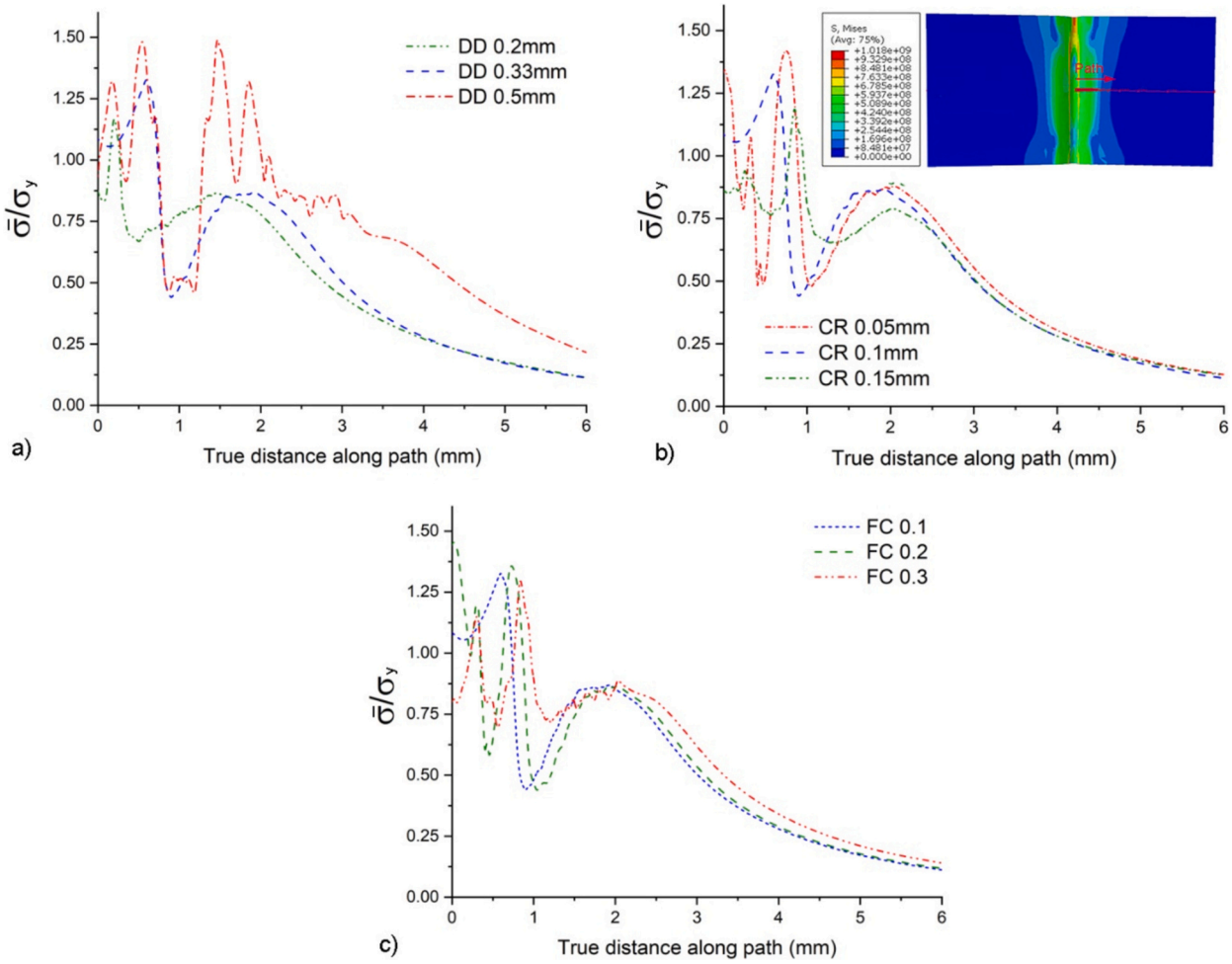

Fig. 15. Variation of stress field in the cross-section of a single channel formed in web direction versus different parameters along the defined path, a) effect of depth of deformation (DD), b) effect of corner radius (CR), and c) effect of friction coefficient (FC).

different points of the sheet could impose a boundary condition. Three points are chosen on the male die to follow their movement path during forming and named point a, b, and c. It is worth mentioning that in order to indicate the forming process clearly, points and their locations are exaggerated. It is assumed that point c is located at its final position of forming and reached the deepest penetration during forming. Point b is next to point c, but it is not involved in forming yet. Once point c starts to unload, point b begins to load at a zone close to it. Hence, because of the presence of point b, material formed by point c cannot be completely free and is clamped somehow by point b. The observation that surrounding material within the channel constrains the forming material (though not completely) necessitates the use of solid elements in the forming simulation. It also has consequences on the degree of plasticity and spring back that are experienced in the rolling versus web directions.

An increase in channel height, associated with a higher male die, leads to greater horizontal movement of the contact points on the dies during the forming process. This means that the male die pushes the sheet further against the wall of the female die, enhancing conformity. In a different way, the channel width does not influence horizontal movement regardless of the forming direction, as points A and B, shown in Fig. 9, remain on the same diameter. However, the spacing between points A and B, which represents the channel width, determines when they participate in the forming process. For narrow channels, points A and B engage in forming almost one after the other, resulting in stress concentration. This close engagement offers more plastic deformation, which can increase the potential for material failure.

3.2. *Verification of modelling*

To verify results of simulations, the thickness reduction resulting from modelling is compared with the experiments in six locations. Fig. 11 shows that 3D modelling of rotary forming produces errors of less than 6 % for all critical locations for channels formed in the web direction. Also, the final overall shape of cross-sections shows a good agreement of simulation and experiment in web direction. Thinning is defined as difference between final and initial thickness divided by initial thickness as follow:

$$\text{Thinning} = \left|\frac{t_f - t_i}{t_i}\right| \tag{2}$$

where t_f and t_i represent final and initial thickness, respectively.

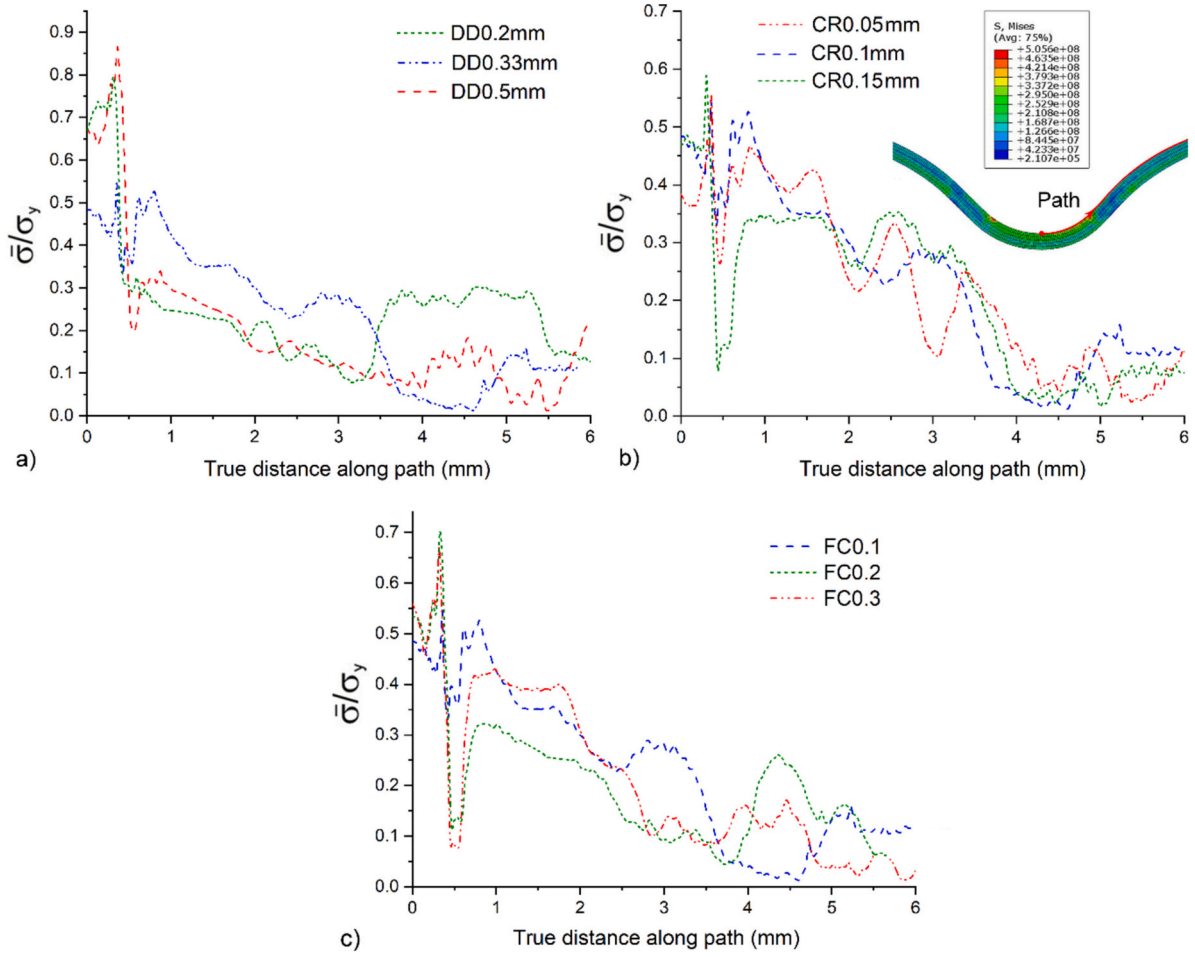

Fig. 16. Variation of stress field in the cross-section of a single channel formed in cross-web direction versus different parameters along the defined path, a) effect of depth for deformation (DD), b) effect of corner radius (CR), and c) effect of friction coefficient (FC).

In Fig. 12, the modelling of cross-web rotary forming is verified with the experimental results. As shown, simulation of rotary forming could predict the process well with thickness error less than 7 %. Both overall shapes of the cross-section of formed sheets and thickness error for different locations resulted from simulation have an appropriate accordance with experiment. Hence, assessing the rotary forming process parameters could be conducted through the current simulation.

In addition to verifying the thinning of the formed sheet at the critical points, the channel height and angle are also taken into account. Fig. 13 shows the variation of channel height and angle in both the web and cross-web directions. The results of three experiments, presented with their average values and error bars, demonstrate good agreement between the experiments and the model in both directions.

3.3. Stress and strain fields

During any forming process, fields of stress and strain are induced into the sheet. Such fields may become important when superimposed with service loading. In rotary forming, two directions of web and cross-web indicate different stress and strain histories. In the cross-web condition, the sheet is formed simultaneously over the entire length of the channel, while in the web direction, the trough is formed incrementally as the sheet moves between the dies. Furthermore, as is shown in Fig. 14, a certain degree of pre-forming occurs, in which the sheet is bent before initial contact with the dies. Ahead of the part is being formed; the sheet is under pre-forming gradually and continuously. As more length of die is involved, forming of a channel occurs in a longer time, so the strain rate is lower, thus leading to more formability. Generally, multi-stage forming would allow more plastic deformation, as well as improving dimensional accuracy [11].

As can be seen in Fig. 14, the material is yielding far from the trough of the female die. In the real bipolar plates, there are several channels parallel to each other, so each channel could affect other channels. In other words, each channel could play the role of a draw bead for other channels around it. To better understand how stresses around a single channel can propagate, the magnitude of the von Mises stress is investigated; this is shown as a function of depth of deformation, corner radius, and friction coefficient in Fig. 15. The ratio of von Mises to yielding stress is reported in the figure when the forming is fully completed. For this material at this strain rate, the ultimate tensile stress is more than three times the yield stress, and this material hardens considerably during deformation. Therefore, this non-dimensional parameter of von Mises stress divided by yield stress can be seen as a measure of the degree of plastic deformation. As shown, the ratio increases with increasing depth of deformation as more plastic deformation is applied into the sheet during forming. Also, increasing the corner

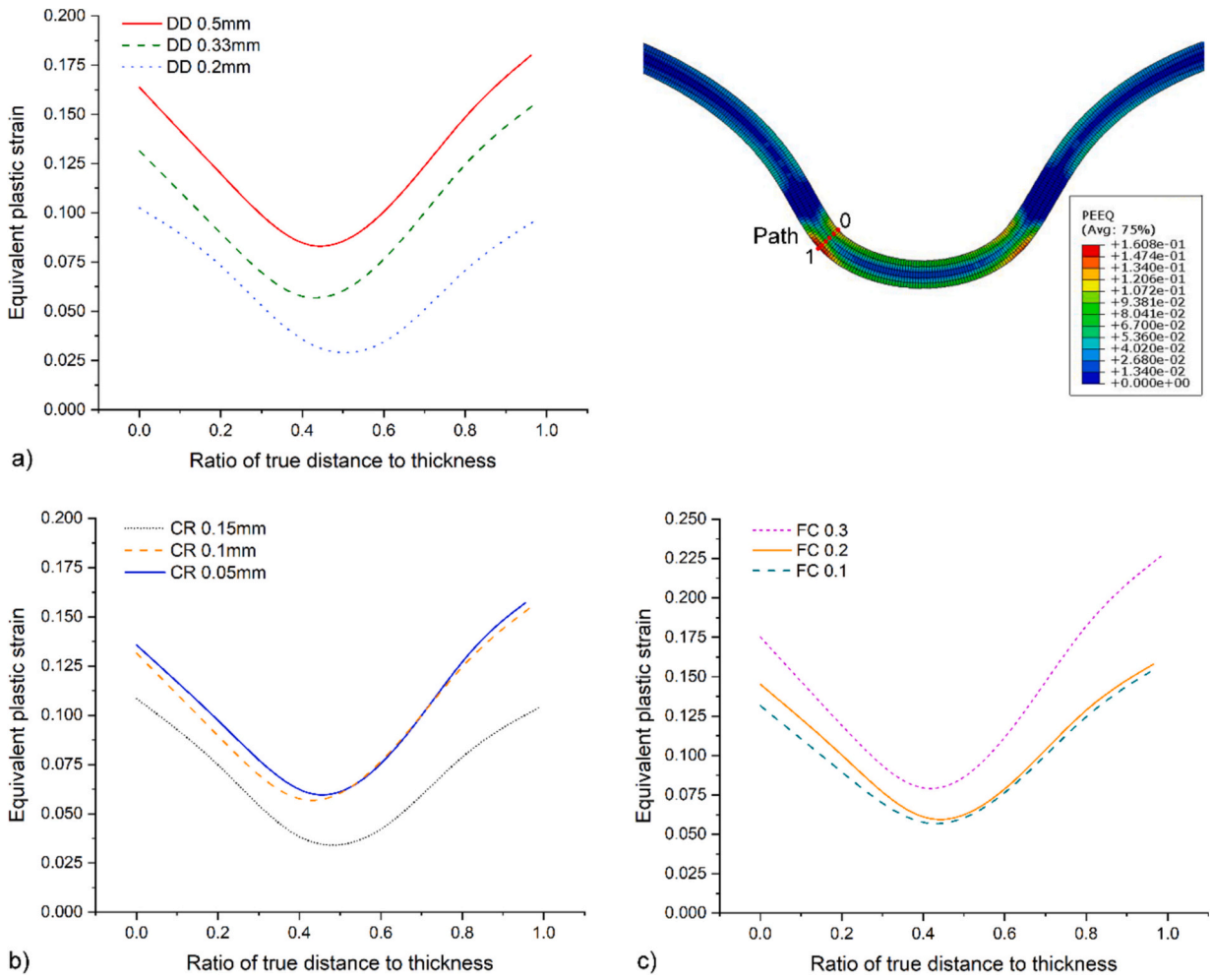

Fig. 17. Effect of process parameters on the critical equivalent plastic strain in cross-web direction, a) effect of depth of deformation (DD), b) effect of corner radius (CR), and c) effect of friction coefficient (FC).

radius was revealed to be an effective approach for reducing the magnitude of the von Mises stress. Similarly, the friction coefficient changes the ratio. In practice, change in friction coefficient is caused by the surface roughness of sheet and rollers leading to the application of more plastic deformation. Generally, the ratio of von Mises stress to yielding stress in the web direction is high (more than one), and it brings the idea that there are some residual stresses caused by self-clamping restricted material deformation.

The ratio of von Mises stress to yielding stress for cross-web direction is shown in Fig. 16. The results are extracted when the forming process is fully completed. As illustrated, the values are much lower than what was observed in web direction. The maximum von Mises stress in the cross-web direction was observed at depth of deformation 0.5 mm, as illustrated in Fig. 16-a. Also, an increase of corner radius from 0.05 to 0.1 mm did not affect the highest peak of the normalized von Mises stress. The highest peak represents the critical zone at the bottom corner of the channel. The friction coefficient generally increased the critical von Mises. The simulations showed that the maximum von Mises stress increases with increasing depth of deformation, decrease of corner radius and increase of friction coefficient.

Equivalent plastic strain was also evaluated, focussing especially on critical areas located on the corner of formed parts. Fig. 17 illustrates the effect of depth of deformation, corner radius, and friction coefficient on the equivalent plastic strain at the most critical location for the channel formed in cross-web direction. As shown, increase in the depth of deformation applies more plastic strain into the sheet. Also, the middle of the thickness experiences low plastic strain compared to the top and bottom, which is to be anticipated from bending-dominated deformation. Lower corner radii (thus, higher thickness to radius ratios) are shown to result in higher strains, which is to be expected from kinematics. As shown in the figure, equivalent plastic strain increases by around 90 % by decreasing the corner radius from 0.15 mm to 0.05 mm. More plastic strain would lead to a risk of material failure. Friction coefficient also changes the equivalent plastic strain. As the male die contacts the sheet, the increase in the friction coefficient would give rise to more plastic strain. It seems that increase in friction coefficient from 0.1 to 0.2 does not change the plastic strain significantly, but more than 0.2 appears to further increase the plastic strain.

Changing from cross-web to web directions varies the pattern of equivalent plastic strain across the thickness. In the cross-web direction, the top and bottom layers of the sheet experience more plastic strain. However, in the web direction as shown in Fig. 18, moving from the top

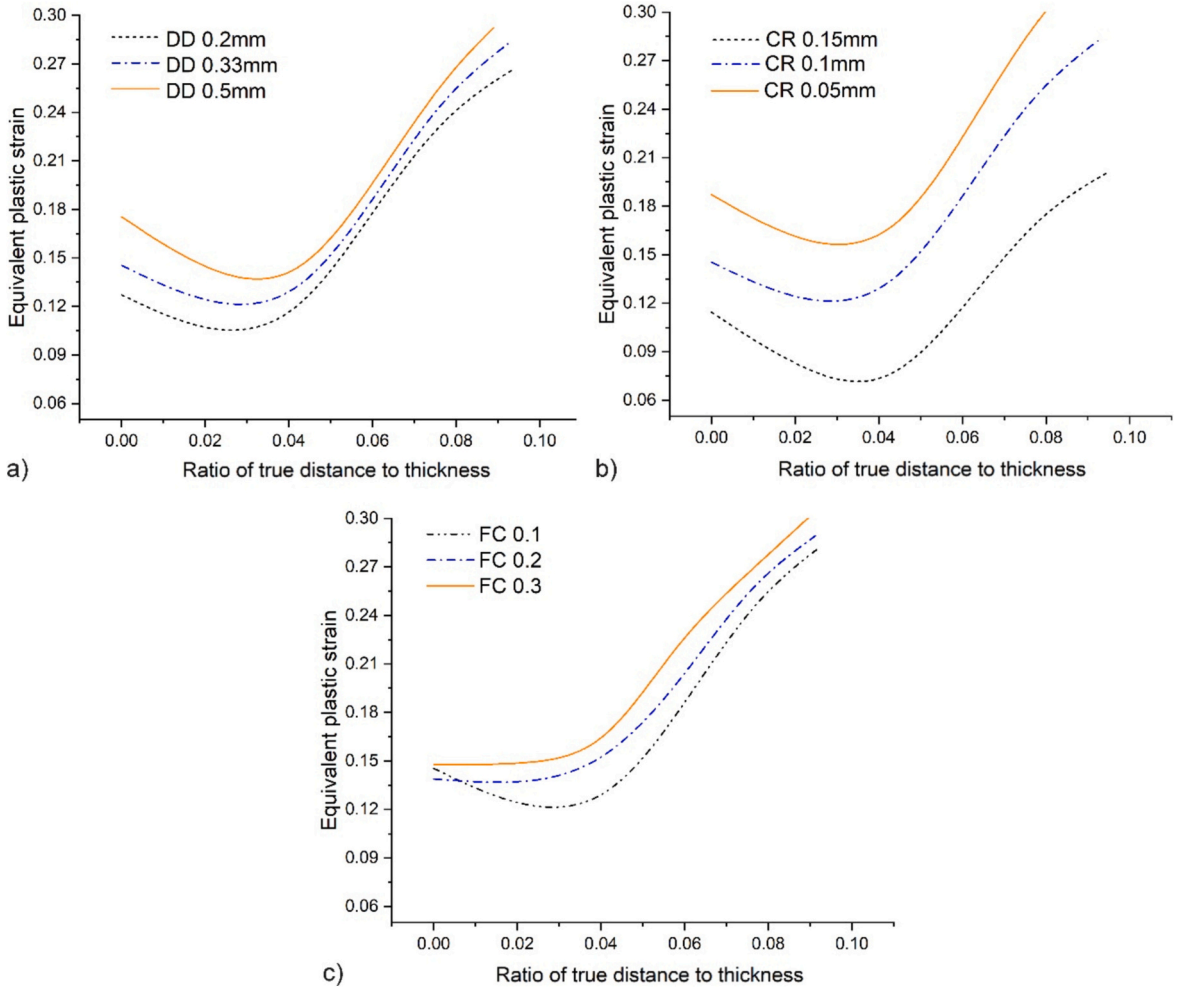

Fig. 18. Effect of process parameters on the equivalent plastic strain of the critical location in web direction, a) effect of depth of deformation (DD), b) effect of corner radius (CR), and c) effect of friction coefficient (FC).

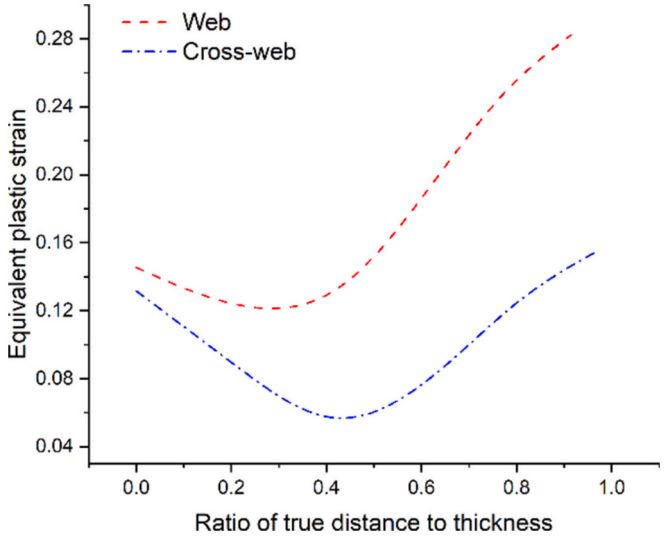

Fig. 19. Comparing equivalent plastic strain along thickness of web and cross-web conditions for depth of deformation 0.33 mm and friction coefficient 0.2.

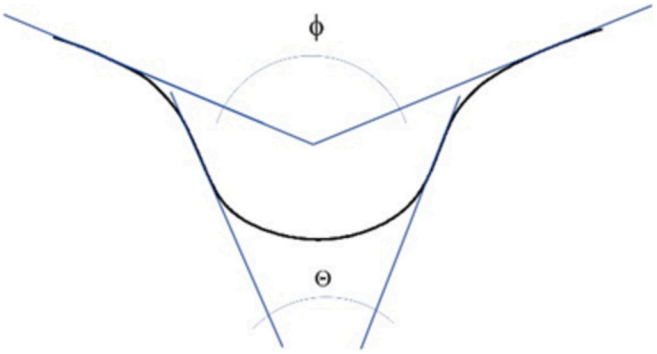

Fig. 20. Schematic of flatness (φ) and channel (Θ) angles in a formed channel.

to bottom would cause an approximate increase in the equivalent strain. This change could be attributed to the increase of membrane strain caused by tension. As a matter of fact, in the web forming, higher ratio of membrane to bending strain is experienced by sheet. Applying more tension happening during web direction could shift the location of neutral axis.

Fig. 19 shows how cross-web and web directions induce different

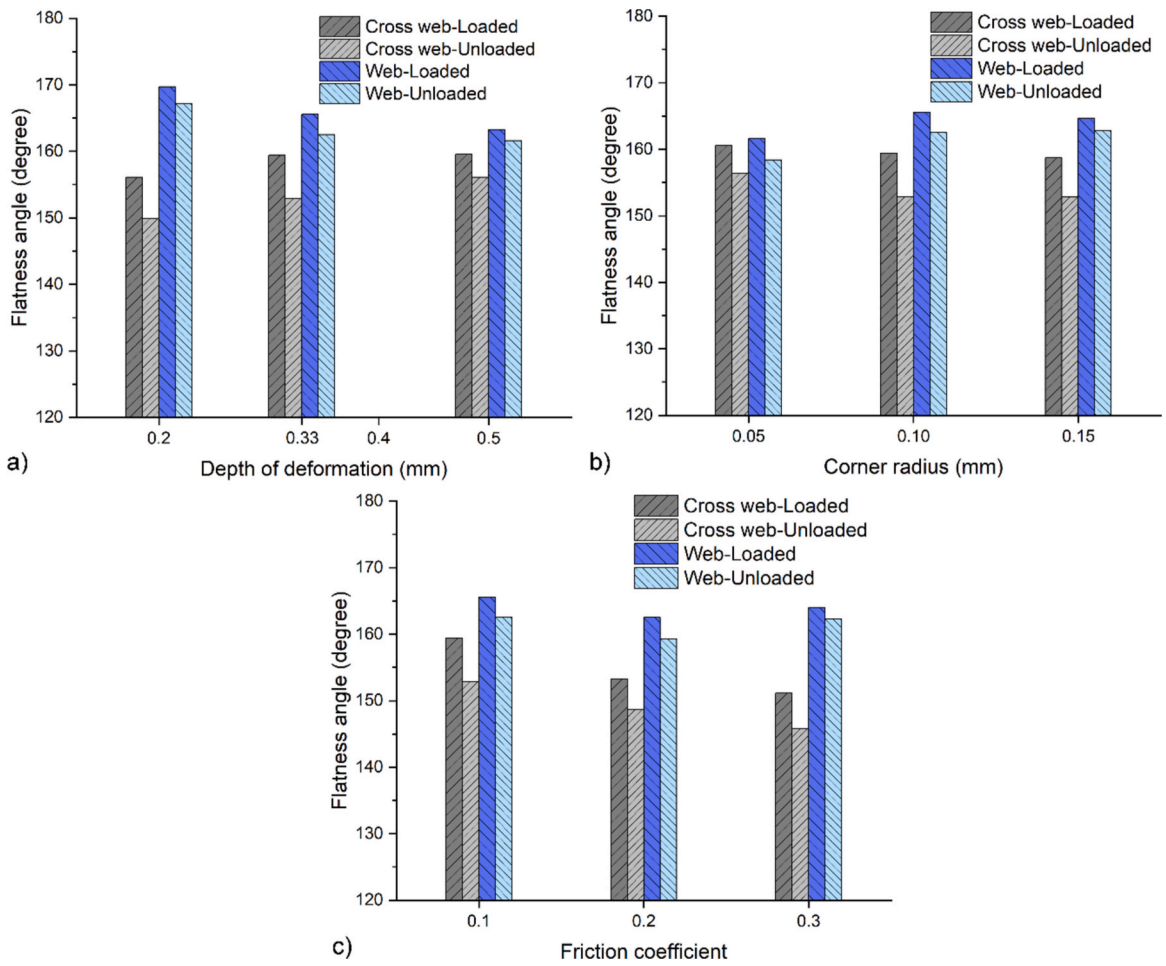

Fig. 21. Effect of forming parameters on the flatness angle, a) depth of deformation effect, b) corner radius effect, and c) friction coefficient effect.

equivalent plastic strain into the sheet. As illustrated, equivalent plastic strain of web direction reaches higher values compared with cross-web direction.

3.4. Channel angles

In this section, the angle of the formed channel is taken into consideration, and the effect of process parameters for both web and cross-web directions are assessed. In this regard, change in the angles of flatness φ and channel Θ, shown schematically in Fig. 20, are evaluated. As mentioned in the introduction, lower channel angles correlate to greater fuel cell performance [38]. Flatness angles approaching 180° make the subsequent processes like welding and assembly of bipolar plates easier [39].

Fig. 21 indicates how forming parameters affect the flatness angle. The loading condition refers to the point when the male die reaches its deepest position, while the unloading condition marks the moment when the forming process is fully complete, and there is no contact between male and sheet surface. The first point attracting attentions is the higher flatness angles of web direction compared with the cross-web direction. The flatness angle increases with depth of deformation for cross web and decreases for the web direction. The corner radius of the die changes the flatness angle, but the dependency is subtle and nonmonotonic. The friction coefficient also changes the flatness angle in the cross-web direction so that more friction coefficient led to less flatness angle. However, the flatness angle for web direction forming is not significantly affected by the friction coefficient. According to the figure, if more flatness angle is desired, less depth of deformation and more die corner radius are recommended in the die design. Comparing the flatness angle of web and cross-web directions when loading and unloading, it is observed that the channels formed in web direction feature less spring back.

What is observed for the effect of depth of deformation on the flatness angle, shown in Fig. 21, is totally different from the channel angle, illustrated in Fig. 22. Forming deeper channels considerably decreases the channel angle regardless of the channel orientation. Forming in the web direction reduced the channel angle remarkably. Having a lower channel angle in the web direction could enhance the performance of fuel cells [38]. Forming in the web direction is less affected by changes in the friction coefficient compared to the cross-web direction. It could be a positive point since during the forming process, the friction coefficient of dies might change gradually due to scratches that are caused by the contacts while forming. Also, channel angles in the web direction are not affected considerably by corner radius. Comparison of the channel angles of loaded and unloaded conditions brings the conclusion that the forming in web direction gives rise to less spring back.

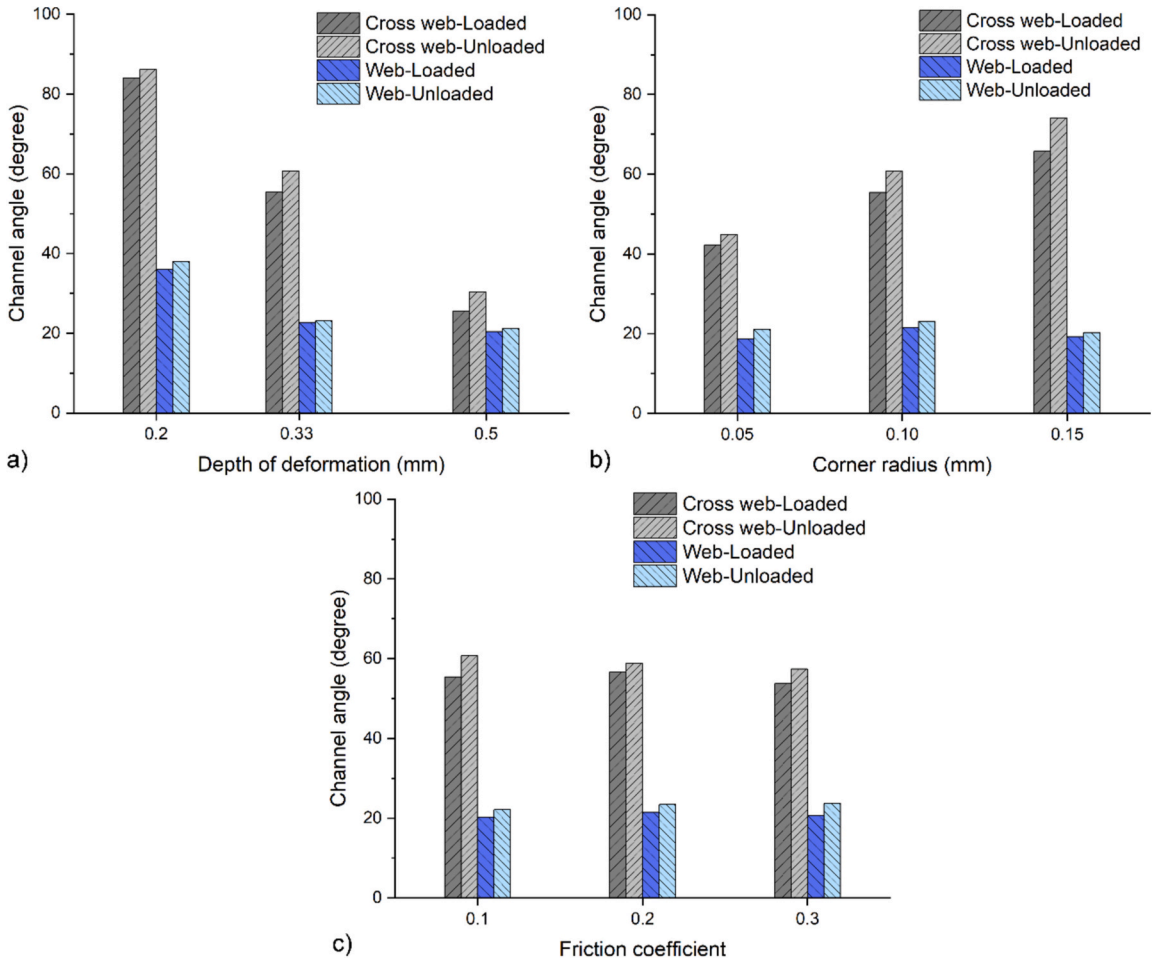

Fig. 22. Effect of forming parameters on the channel angle, a) depth of deformation effect, b) corner radius effect, and c) friction coefficient effect.

3.5. *Thickness distribution*

The thickness distribution for the cases of web and cross-web directions is shown in Fig. 23. In this figure, the numbering convention of the locations is the same as in Fig. 12. As can be seen, higher depth of deformation reduces the thickness due to increased membrane strains during the forming process. The figure shows that in the web direction, as sheet in the forming zone is controlled or restricted by other materials around it, more thinning occurs. In other words, the sheet itself is playing the role of holder. Comparing the thickness distribution of web and cross-web forming cases indicates that the cross-web direction gives rise to a more uniform distribution. Thinning is seen in the corners of die locations 3 and 4 because this is the area that is required to have the greatest membrane strain in order to conform to the penetration of the male die. Also, from the figure, it is concluded that dies with lower corner radius impose more thinning into the material. Generally, lower corner radius increases the bending strains and stress concentration. Likewise, the friction coefficient affects the final thickness corresponding to the forces acting between die and sheet surface. This force could apply some tension leading to more plastic deformation and thinning in final formed sheets. The friction coefficient is not a significant parameter compared with others. In particular, changing the surface friction coefficient from 0.1 to 0.3 does not have a valuable effect on the final thickness although some small changes are observed. In reality, friction coefficient results from the surface roughness of as-received sheets, and the forming process could be controlled using lubricants. In the case of bipolar plates, as using lubricants might require additional manufacturing steps like cleaning of sheet surface after forming, the requirement to reduce the friction coefficient can increase the manufacturing cost.

4. Conclusions

In this paper, the effects of several important parameters (namely, depth of deformation, corner radius, and friction coefficient) are evaluated for the rotary forming process of SS316L. Two different orientations of channels are taken into consideration. The following conclusions can be drawn:

- In the forming process along the web direction, the sheet experiences some pre-deformation before its first contact with the die, followed by additional deformation between the initial contact and full

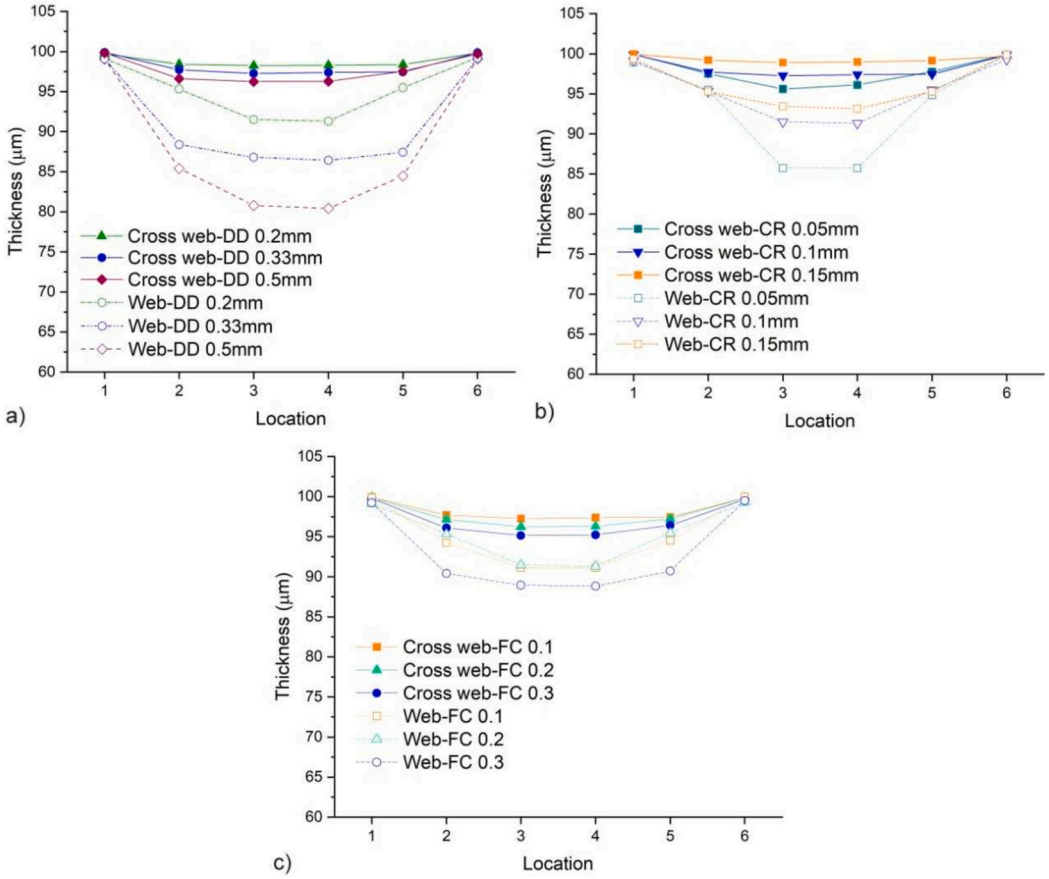

Fig. 23. Effect of the rotary forming parameters on the thickness distribution, a) effect of depth of deformation, b) effect of corner radius, and c) effect of friction coefficient.

shaping. Preforming typically enhances formability. Additionally, forming in the web direction is a continuous process that moves along the channel. In contrast, in the cross-web direction, forming happens over the entire length of the channel simultaneously, with little or no pre-deformation occurring.

- Von Mises stresses tend to be higher when the channel is formed in the web direction when compared to the cross-web direction. In addition to the increased von Mises stress in the web direction, a larger area is subjected to high stresses when forming occurs in this direction.
- The sheets formed in the web direction undergo greater equivalent plastic strain compared to those formed in the cross-web direction. Specifically, when the depth of deformation is 0.33 mm and the friction coefficient is 0.2, the entire thickness of the sheet experiences more plastic deformation in the web direction than in the cross-web direction.
- An increase in the depth of deformation, the presence of sharper corners, and a higher friction coefficient result in greater plastic stresses and strains.
- Forming in the web direction produces better conformity to desired shapes since it would lead to higher flatness angle and lower channel angle. This might affect subsequent processes like welding and assembly of fuel cells. The friction coefficient is not a significant parameter compared to depth of deformation and corner radius in terms of effects on the channel angle.
- Thickness reduction is more significant in web-direction forming compared to cross-web direction, indicating a higher risk of failure in the web direction. Also, depth of deformation and corner radius are the main effective parameters on the thinning of sheet.

CRediT authorship contribution statement

A. Asgari: Methodology, Investigation. **M. Zeestraten:** Investigation, Funding acquisition. **C.L. Walters:** Supervision.

Declaration of competing interest

The authors declare that they have no known competing financial interests or personal relationships that could have appeared to influence the work reported in this paper.

Acknowledgment

The authors would like to express their sincere gratitude to Madern Tooling Group and TKI Nieuw Gas, who have supported the research financially.

References

[1] Sudarsan C, Prasad KS, Hazra S, Panda SK. Forming of serpentine micro-channels on SS304 and AA1050 ultra-thin metallic sheets using stamping technology. Journal of Manufacturing Processes 2020;56:1099–113.
[2] Wang X-D, Yan W-M, Duan Y-Y, Weng F-B, Jung G-B, Lee C-Y. Numerical study on channel size effect for proton exchange membrane fuel cell with serpentine flow field. Energ Conver Manage 2010;51:959–68.
[3] Kerkoub Y, Benzaoui A, Haddad F, Ziari YK. Channel to rib width ratio influence with various flow field designs on performance of PEM fuel cell. Energ Conver Manage 2018;174:260–75.
[4] Manso A, Marzo F, Mujika MG, Barranco J, Lorenzo A. Numerical analysis of the influence of the channel cross-section aspect ratio on the performance of a PEM fuel cell with serpentine flow field design. Int J Hydrogen Energy 2011;36:6795–808.

[5] Leng Y, Ming P, Yang D, Zhang C. Stainless steel bipolar plates for proton exchange membrane fuel cells: materials, flow channel design and forming processes. J Power Sources 2020;451:227783.
[6] Modanloo V, Talebi-Ghadikolaee H, Alimirzaloo V, Elyasi M. Fracture prediction in the stamping of titanium bipolar plate for PEM fuel cells. Int J Hydrogen Energy 2021;46:5729–39.
[7] Talebi-Ghadikolaee H, Elyasi M, Seddighi S, Khatir FA, Modanloo V. Characterization and prediction of micro channel depth of ultra-thin bipolar plates for PEMFCs. Journal of Engineering Research 2024.
[8] Bell C, Corney J, Zuelli N, Savings D. A state of the art review of hydroforming technology: its applications, research areas, history, and future in manufacturing. International Journal of Material Forming 2020;13:789–828.
[9] Kargar-Pishbijari H, Hosseinipour SJ, Aval HJ. A novel method for manufacturing microchannels of metallic bipolar plate fuel cell by the hot metal gas forming process. Journal of Manufacturing Processes 2020;55:268–75.
[10] Wu M, Lu C, Wen D. Materials and manufacture methods for bipolar plates of PEMFC. Materials Research Innovations 2015;19 [S8-85-S88-88].
[11] Tran MT, Lee DH, Lee HW, Kim D-K. Formability improvement in multi-stage stamping of ultra-thin metallic bipolar plate for proton exchange membrane fuel cell. Int J Hydrogen Energy 2022;47:40008–25.
[12] Talebi-Ghadikolaee H, Modanloo V, Elyasi M, Khatir FA. Multiple criteria decision support analysis for manufacturing process parameters selection of metallic bipolar plates for polymer electrolyte membrane fuel cells. Proceedings of the Institution of Mechanical Engineers, Part L: Journal of Materials: Design and Applications 2024; 238:929–42.
[13] Xu S, Li K, Wei Y, Jiang W. Numerical investigation of formed residual stresses and the thickness of stainless steel bipolar plate in PEMFC. Int J Hydrogen Energy 2016;41:6855–63.
[14] Hu Q, Zhang D, Fu H, Huang K. Investigation of stamping process of metallic bipolar plates in PEM fuel cell—numerical simulation and experiments. Int J Hydrogen Energy 2014;39:13770–6.
[15] Karacan K, Celik S, Toros S, Alkan M, Aydin U. Investigation of formability of metallic bipolar plates via stamping for light-weight PEM fuel cells. Int J Hydrogen Energy 2020;45:35149–61.
[16] Teng F, Wang H, Shi S, Li J, Sun J, Sun J, et al. Shape and position design of two-step micro-channel on plate during rubber pad forming process based on simulation. The International Journal of Advanced Manufacturing Technology 2022;121:753–63.
[17] Qiu D, Peng L, Yi P, Lai X, Lehnert W. Flow channel design for metallic bipolar plates in proton exchange membrane fuel cells: experiments. Energ Conver Manage 2018;174:814–23.
[18] Mahabunphachai S, Cora ÖN, Koç M. Effect of manufacturing processes on formability and surface topography of proton exchange membrane fuel cell metallic bipolar plates. J Power Sources 2010;195:5269–77.
[19] Chen T-C, Ye J-M. Fabrication of micro-channel arrays on thin stainless steel sheets for proton exchange membrane fuel cells using micro-stamping technology. The International Journal of Advanced Manufacturing Technology 2013;64:1365–72.
[20] Chen T-C, Ye J-M. Analysis of stainless steel bipolar plates micro-stamping processes. Prz Elektrotechniczn 2012;88:121–6.
[21] Gao H, Lan J, Hua L. Deformation prediction of the bipolar plate stamping. In: Advanced materials research. Trans Tech Publ; 2014. p. 270–4.
[22] Jin C, Jeong M, Kang C. Effect of process parameters on forming depth of channels in fuel cell bipolar plates fabricated using rubber forming process. Materials Research Innovations 2014;18 [S2-467-S462-472].
[23] Porstmann S, Wannemacher T, Drossel W-G. A comprehensive comparison of state-of-the-art manufacturing methods for fuel cell bipolar plates including anticipated future industry trends. Journal of Manufacturing Processes 2020;60:366–83.
[24] Nikam VV, Reddy RG. Corrugated bipolar sheets as fuel distributors in PEMFC. Int J Hydrogen Energy 2006;31:1863–73.
[25] Xu C, Wei Y, Pan T, Chen J. A study of cold roll forming technology and peak strain behavior of asymmetric corrugated channels. The International Journal of Advanced Manufacturing Technology 2022:1–11.
[26] Abeyrathna B, Zhang P, Pereira MP, Wilkosz D, Weiss M. Micro-roll forming of stainless steel bipolar plates for fuel cells. Int J Hydrogen Energy 2019;44:3861–75.
[27] Bauer A, Härtel S, Awiszus B. Manufacturing of metallic bipolar plate channels by rolling. Journal of Manufacturing and Materials Processing 2019;3:48.
[28] P. Zhang, M. Pereira, B. Rolfe, W. Daniel, M. Weiss, Deformation in micro roll forming of bipolar plate, in: Journal of physics: conference series, IOP Publishing, 2017, pp. 012115.
[29] Huang J, Deng Y, Yi P, Peng L. Experimental and numerical investigation on thin sheet metal roll forming process of micro channels with high aspect ratio. The International Journal of Advanced Manufacturing Technology 2019;100:117–29.
[30] Xu Z, Huang J, Mao M, Peng L, Lai X. An investigation on the friction in a micro sheet metal roll forming processes considering adhesion and ploughing. J Mater Process Technol 2020;285:116790.
[31] Ren M, Lin F, Jia F, Xie H, Yang M, Jiang Z. Micro rolling fabrication of copper/SS304L micro composite channels. Journal of Manufacturing Processes 2023;90: 1–13.
[32] Wang J, Sun J, Li S, Wen Z, Ji S. Surface diffusion modification AISI 304SS stainless steel as bipolar plate material for proton exchange membrane fuel cell. Int J Hydrogen Energy 2012;37:1140–4.
[33] Cho K, Lee W, Lee S, Jang H. Corrosion resistance of chromized 316L stainless steel for PEMFC bipolar plates. J Power Sources 2008;178:671–6.
[34] Guo N, Hou Z, Wang W, Zhang X, Yang D, Min J, et al. Flow stress modeling of ultra-thin austenitic stainless steel for proton exchange membrane fuel cell incorporating strain rate, temperature, and grain size. J Mater Process Technol 2023;319:118099.
[35] Langdon G, Schleyer G. Unusual strain rate sensitive behaviour of AISI 316L austenitic stainless steel. The Journal of Strain Analysis for Engineering Design 2004;39:71–86.
[36] Haroush S, Priel E, Moreno D, Busiba A, Silverman I, Turgeman A, et al. Evaluation of the mechanical properties of SS-316L thin foils by small punch testing and finite element analysis. Materials & Design 2015;83:75–84.
[37] Asgari A, Dehestani P, Poruraminaie I. On the residual stress modeling of shot-peened AISI 4340 steel: finite element and response surface methods. Mechanics & Industry 2017;18:605.
[38] Wilberforce T, El Hassan Z, Ogungbemi E, Ijaodola O, Khatib F, Durrant A, et al. A comprehensive study of the effect of bipolar plate (BP) geometry design on the performance of proton exchange membrane (PEM) fuel cells. Renew Sustain Energy Rev 2019;111:236–60.
[39] Peng L, Yi P, Lai X. Design and manufacturing of stainless steel bipolar plates for proton exchange membrane fuel cells. Int J Hydrogen Energy 2014;39:21127–53.